



# Adenosine A<sub>1</sub> receptor activates background potassium channels and modulates information processing in olfactory bulb mitral cells

Natalie Rotermund<sup>1</sup>, Svenja Winandy<sup>1</sup>, Timo Fischer<sup>1</sup>, Kristina Schulz<sup>1</sup>, Torsten Fregin<sup>1</sup>, Nadine Alstedt<sup>1</sup>, Melanie Buchta<sup>1</sup>, Janick Bartels<sup>1</sup>, Mattias Carlström<sup>2</sup> , Christian Lohr<sup>1</sup>  and Daniela Hirnet<sup>1</sup>

<sup>1</sup>Division of Neurophysiology, Institute of Zoology, University of Hamburg, Martin-Luther-King-Platz 3, Hamburg, 20146, Germany

<sup>2</sup>Department of Physiology and Pharmacology, Karolinska Institutet, Nanna Svartz Väg 2, Stockholm, 17177, Sweden

Edited by: Yoshihiro Kubo & Takashi Kurahashi

## Key points

- Adenosine is a widespread neuromodulator in the mammalian brain, but whether it affects information processing in sensory system(s) remains largely unknown.
- Here we show that adenosine A<sub>1</sub> receptors hyperpolarize mitral cells, one class of principal neurons that propagate odour information from the olfactory bulb to higher brain areas, by activation of background K<sup>+</sup> channels.
- The adenosine-modulated background K<sup>+</sup> channels belong to the family of two-pore domain K<sup>+</sup> channels.
- Adenosine reduces spontaneous activity of mitral cells, whereas action potential firing evoked by synaptic input upon stimulation of sensory neurons is not affected, resulting in a higher ratio of evoked firing (signal) over spontaneous firing (noise) and hence an improved signal-to-noise ratio.
- The study shows for the first time that adenosine influences fine-tuning of the input–output relationship in sensory systems.

**Abstract** Neuromodulation by adenosine is of critical importance in many brain regions, but the role of adenosine in olfactory information processing has not been studied so far. We investigated the effects of adenosine on mitral cells, which are projection neurons of the olfactory bulb. Significant expression of A<sub>1</sub> and A<sub>2A</sub> receptors was found in mitral cells, as demonstrated by *in situ* hybridization. Application of adenosine in acute olfactory bulb slices hyperpolarized mitral cells in wild-type but not in adenosine A<sub>1</sub> receptor knockout mice. Adenosine-induced hyperpolarization was mediated by background K<sup>+</sup> currents that were reduced by halothane and

**Natalie Rotermund** received her PhD in Neurophysiology from the University of Hamburg. After working in the medical device industry for some years, she decided to return to university and follow her interest in fundamental research. She is currently employed as postdoctoral researcher in the Division of Neurophysiology at the University of Hamburg. Her research focuses on the understanding of purinergic signalling in the central nervous system, with a specialization in electrophysiological and imaging techniques.



C. Lohr and D. Hirnet contributed equally.

bupivacaine, which are known to inhibit two-pore domain K<sup>+</sup> (K2P) channels. In mitral cells, electrical stimulation of axons of olfactory sensory neurons evoked synaptic currents, which can be considered as input signals, while spontaneous firing independent of sensory input can be considered as noise. Synaptic currents were not affected by adenosine, while adenosine reduced spontaneous firing, leading to an increase in the signal-to-noise ratio of mitral cell firing. Our findings demonstrate that A<sub>1</sub> adenosine receptors activate two-pore domain K<sup>+</sup> channels, which increases the signal-to-noise ratio of the input–output relationship in mitral cells and thereby modulates information processing in the olfactory bulb.

(Resubmitted 31 October 2017; accepted after revision 7 December 2017; first published online 22 December 2017)

**Corresponding authors** C. Lohr and D. Hirnet: Division of Neurophysiology, Institute of Zoology, Martin-Luther-King-Platz 3, Hamburg, 20146, Germany. Emails: christian.lohr@uni-hamburg.de & daniela.hirnet@uni-hamburg.de

## Introduction

Adenosine is a ubiquitous neuromodulator involved in many physiological processes such as sleep, memory formation, synaptic plasticity and neuronal excitability, but also in the pathophysiology of the brain (Fredholm *et al.* 2005; Boison, 2009; Ribeiro & Sebastiao, 2010; Dias *et al.* 2013). There are four adenosine receptors cloned, A<sub>1</sub>, A<sub>2A</sub>, A<sub>2B</sub> and A<sub>3</sub>, all of them being G-protein-coupled receptors. While A<sub>1</sub> and A<sub>3</sub> receptors are coupled to G<sub>i</sub> proteins, A<sub>2A</sub> and A<sub>2B</sub> are linked to G<sub>s</sub> proteins. A<sub>1</sub> and A<sub>2A</sub> receptors are widespread in the brain and often exert opposing effects on neuronal performance (Cunha, 2005). In the hippocampus, for example, A<sub>1</sub> receptors mediate synaptic attenuation by inhibition of presynaptic calcium channels, while A<sub>2A</sub> receptors counteract this effect by a protein kinase C-dependent mechanism (Lopes *et al.* 2002; Gundlfinger *et al.* 2007). A<sub>1</sub> receptors have also been shown to decrease neuronal excitability by activation of G-protein-coupled inwardly rectifying potassium channels (GIRKs; Sickmann & Alzheimer, 2003; Kim & Johnston, 2015). GIRKs are targets of A<sub>1</sub> receptors in the retina, where they mediate hyperpolarization and a reduction in action potential firing in ganglion cells elicited by light stimulation of photoreceptor cells (Clark *et al.* 2009). While the role of adenosine in the retina is well documented (for a review, see Dos Santos-Rodrigues *et al.* 2015), it is not known if and how adenosine receptors affect the input–output relation of sensory information in other brain areas dedicated to sensory information processing (Housley *et al.* 2009; Lohr *et al.* 2014).

First evidence suggests a neuromodulatory role of adenosine receptors in the olfactory bulb. The A<sub>2A</sub> receptor, for example, has been demonstrated by radioligand binding, *in situ* hybridization and antibody staining (Johansson *et al.* 1997; Rosin *et al.* 1998; Kaelin-Lang *et al.* 1999). Olfactory sensory axons might be the source of adenosine since they release ATP as a cotransmitter (Thyssen *et al.* 2010). ATP excites mitral cells via P2Y<sub>1</sub> receptors (Fischer *et al.* 2012), is then degraded to

adenosine and elicits calcium transients in astrocytes expressing A<sub>2A</sub> receptors, emphasizing a physiological relevance of adenosine in this brain area (Doengi *et al.* 2008). In addition, adenosine derived from ATP released from astrocytes modulates slow membrane potential oscillations of olfactory bulb mitral cells (Roux *et al.* 2015). The mechanism by which adenosine modulates mitral cells and whether adenosine affects odour information processing, however, remain to be shown. We found that activation of A<sub>1</sub> receptors hyperpolarizes mitral cells by opening of two-pore domain potassium (K2P) channels, thereby decreasing spontaneous firing activity. The firing frequency of mitral cells upon synaptic stimulation via olfactory sensory axons, in contrast, remains unaffected by adenosine, resulting in a higher ratio of evoked firing (signal) over spontaneous firing (noise) and hence an improved signal-to-noise ratio.

## Methods

### Ethical approval

Animal rearing, dissection and all experiments were performed according to the European Union's and German animal welfare guidelines and were approved by the local authorities (GZ G21305/591-00.33; Behörde für Gesundheit und Verbraucherschutz, Hamburg, Germany). They conform to the principles and regulations described by Grundy (2015). Mice of both sexes (age: postnatal days 8–21) were anaesthetized with isoflurane and decapitated.

### Animals and preparation procedure

Naval Medical Research Institute (NMRI) outbred mice, OMP-synapto-pHluorin-expressing mice (Bozza *et al.* 2004) and A<sub>1</sub> receptor knockout mice (Johansson *et al.* 2001) were bred in the institute's animal facility (12 h–12 h light–dark cycle, food and water *ad libitum*). Olfactory bulbs were dissected and horizontal brain slices were prepared as described before (Fischer *et al.* 2012).

Olfactory bulbs were quickly transferred into a chilled slicing artificial cerebrospinal fluid (ACSF) that contained (in mM): NaCl, 83; NaHCO<sub>3</sub>, 26.2; NaH<sub>2</sub>PO<sub>4</sub>, 1; KCl, 2.5; sucrose, 70; D-glucose, 20; CaCl<sub>2</sub>, 0.5; MgSO<sub>4</sub>, 2.5. Sagittal slices 200  $\mu$ m thick of the bulbs were cut using a vibrating blade microtome (Leica VT1200S, Bensheim, Germany). Brain slices were stored in ACSF containing (in mM): NaCl, 120; NaHCO<sub>3</sub>, 26; NaH<sub>2</sub>PO<sub>4</sub>, 1; KCl, 2.5; D-glucose, 2.8; CaCl<sub>2</sub>, 2; MgCl<sub>2</sub>, 1. Storage lasted for 30 min at 30°C and 15 min at room temperature before starting experiments. ACSF was continuously gassed with carbogen (95% O<sub>2</sub>–5% CO<sub>2</sub>; buffered to pH 7.4 with CO<sub>2</sub>/bicarbonate).

## Drugs

Adenosine, adenosine-5'-diphosphate, adenosine-5'-triphosphate, barium chloride, halothane and 8-cyclopentyl-1,3-dipropylxanthine (DPCPX) were purchased from Sigma-Aldrich (Munich, Germany); N<sup>6</sup>-cyclopentyladenosine (N<sup>6</sup>-CPA), N-[4-[1-[2-(6-methyl-2-pyridinyl)ethyl]-4-piperidinyl]carbonyl]phenyl]-methanesulfonamide dihydrochloride (E-4031), tetrodotoxin citrate (TTX), 10,10-bis(4-pyridinylmethyl)-9(10H)-anthracenone dihydrochloride (XE 991), 6,12,19,20,25,26-hexahydro-5,27:13,18:21,24-trietheno-11,7-metheno-7H-dibenzo [b,n]-[1,5,12,16]tetraazacyclotricosin-5,13-dium dibromid (UCL 1684) and 4-aminopyridine (4-AP) were from Tocris (Bristol, UK); 2,3-dioxo-6-nitro-1,2,3,4-tetrahydrobenzo-[f]-quinoxaline-7-sulfonamide (NBQX), D-(–)-2-amino-5-phosphonopentanic acid (D-APV) and gabazine hydrobromide were from Abcam (Cambridge, UK); tetramethyl ammonium (TEA) was from Applichem (Darmstadt, Germany); 1-[(2-chlorophenyl)diphenylmethyl]-1H-pyrazole (TRAM-34) was from Alomone Labs (Jerusalem, Israel).

## Electrophysiological recordings

Mitral cells of the main olfactory bulb were investigated using the patch-clamp technique (MultiClamp 700B amplifier and pCLAMP 10 software, Molecular Devices, Biberach, Germany). Throughout the experiments, brain slices were superfused with ACSF. In ACSF with 5 mM K<sup>+</sup> concentration, equimolar amounts of NaCl were replaced by KCl. Drugs were applied with the perfusion system driven by a peristaltic pump (Reglo, Ismatec, Wertheim, Germany) at a flow rate of 2 ml min<sup>-1</sup>. Application of drugs was achieved by manually changing the inflow of the pump from drug-free to drug-containing ACSF. Application bars reflect the time window during which drug-containing ACSF was added to the bath, the time being corrected for the time needed for the drug to pass the tubing and enter the bath. Complete bath exchange required approximately 30 s. If not stated otherwise, the whole-cell configuration was employed using patch

pipettes with a resistance of  $\sim$ 3 M $\Omega$ . Recordings were digitized (Digidata 1440A, Molecular Devices, Biberach, Germany) at 10–20 kHz and filtered (Bessel filter, 2 kHz). The standard pipette solution contained (in mM): NaCl, 10; potassium gluconate, 105; K<sub>3</sub>-citrate, 20; Hepes, 10; MgCl<sub>2</sub>, 0.5; Mg-ATP, 5; Na-GTP, 0.5; mannitol, 21; phosphocreatine, 5. Pipette solution with reduced K<sup>+</sup> concentration contained (in mM): NaCl, 10; K-gluconate, 110; K<sub>3</sub>-citrate, 10; Hepes, 10; EGTA, 0.25; MgCl<sub>2</sub>, 0.5; Mg-ATP, 3; Na-GTP, 0.5. High-chloride pipette solution contained (in mM): NaCl, 10; potassium gluconate, 52.5; KCl, 55; K<sub>3</sub>-citrate, 10; Hepes, 10; EGTA, 0.25; MgCl<sub>2</sub>, 0.5; Mg-ATP, 3; Na-GTP, 0.5. The pipette solutions contained 8  $\mu$ M Alexa Fluor 594 in most of the experiments. For extracellular recordings of action potentials, patch pipettes were filled with ACSF (resistance  $\sim$ 3 M $\Omega$ ) and the cell-attached configuration was established. For stimulation of axons of olfactory sensory neurons we used ACSF-filled pipettes with a resistance of  $\sim$ 2 M $\Omega$ . The stimulation pipette was placed in the olfactory nerve layer at a distance of at least 50  $\mu$ m to the apical dendrite of the recorded mitral cell. Current pulses (100  $\mu$ A, 50  $\mu$ s) were applied to evoke synaptic excitation of mitral cells. In control experiments, synaptic currents were entirely blocked by application of 1  $\mu$ M TTX, confirming that stimulation-induced currents were synaptically evoked, but not evoked by direct stimulation of the mitral cell.

## Measurements of membrane conductance and reversal potential

The membrane conductance was measured in voltage clamp with a holding potential of  $-70$  mV. A hyperpolarizing voltage step of 10 mV and 1 s duration was applied every 10 s and the membrane conductance was calculated from the resulting current shift that was measured at the end of the voltage step. To estimate the reversal potential of the adenosine-induced membrane potential shift, the membrane potential was recorded in current clamp and hyperpolarized by current steps of 500 ms duration and increasing amplitude (50 pA interval) before and during application of adenosine. The difference between membrane potential values recorded before and during adenosine application at a given current step was calculated, and the values of all experiments averaged and plotted against the membrane potential value before adenosine application. All data were pooled and a linear regression was calculated. The point of intersection of the regression line and the abscissa reflects the reversal potential of the adenosine-induced membrane potential shift. The current–voltage relationship of the adenosine-evoked current was obtained by applying voltage ramps (duration: 800 ms) from  $-20$  to  $-130$  mV in the absence and in the presence of adenosine. The difference of the obtained current traces revealed the

adenosine-evoked current. The resulting current–voltage relationship was corrected for a liquid junction potential of  $-18$  mV.

### Synapto-pHluorin recordings

Mice expressing synapto-pHluorin (syn-pH) exclusively in olfactory sensory neurons were employed to study the effect of adenosine on vesicle fusion in olfactory sensory nerve terminals as described in Thyssen *et al.* (2010). Olfactory bulbs *in toto* (Stavermann *et al.* 2015) were placed under a confocal microscope (eCI, Nikon, Düsseldorf, Germany) and syn-pH was excited at 488 nm. Fluorescence was collected using a bandpass filter between 515 and 545 nm. Olfactory sensory axons were stimulated using a stimulation isolator (DS3, Digitimer, Welwyn Garden City, UK). Regions of interest were defined in the glomeruli and changes in the syn-pH fluorescence were calculated with the baseline fluorescence before stimulation taken as 100%.

### A<sub>1</sub> receptor *in situ* hybridization

**Probe design.** mRNA probes for adenosine receptors were designed based upon cDNA clone MGC:90841 (*ADORA1*) and MGC:118414 (*ADORA2A*). For A<sub>1</sub> receptor RNA probes, a sequence was amplified by PCR from cDNA isolated from mouse brain (SuperScript III, Thermo Fisher Scientific, Darmstadt, Germany) using the following primer set: forward: 5'-CGTGTCATGTGAGACCCTTCCTGCTG; reverse: 5'CAGGCTCAATTTCCAAAGCTGGGCTCTG. For A<sub>2A</sub> receptor RNA probes, the following sequences were used: forward: GAAACGCC CACGCCAGGAAACC; reverse: GCAGACGGTCTCTC GGGTTAGC. The sequences were tested for correctness and orientation (GATC, Konstanz, Germany) and cloned into pGEM-T easy vector. Vectors were multiplied, linearized and purified as a basis for labelling and transcription of adenosine receptor RNA probes.

**Hybridization procedure for radiolabelled probes.** For whole brain *in situ* hybridization (ISH), radioactive probes based on the sequence stated above were used. Labelling of [<sup>35</sup>S]UTPs was performed with the Maxiscript Kit (Ambion, Thermo Fisher Scientific) according to the manufacturer's instructions. Brain slices (16  $\mu$ m) on slides were fixed in 4% paraformaldehyde in PBS for 10 min at 4°C. Acetylation was performed for 10 min in triethanolamine (0.1 M), 0.9% NaCl solution and acetic anhydride (2.5 ml l<sup>-1</sup>) in PBS, followed by dehydration in ethanol (60/80/90/95/99.8%). Prehybridization buffer (50% deionized formamide, 5 $\times$  hybridization salts (750 mM NaCl, 25 mM PIPES, 25 mM EDTA, pH 6.8), 5 $\times$  Denhardt's solution (0.05% Ficoll, 0.05% polyvinylpyrrolidone, 0.1% BSA), 0.02% SDS, 10 mM DTT,

10% dextran sulfate, 250  $\mu$ g ml<sup>-1</sup> herring-sperm DNS, 250  $\mu$ g ml<sup>-1</sup> yeast tRNA) was incubated on slides at 50°C for 2 h in a humidity chamber. Hybridization was performed with 2  $\times$  10<sup>6</sup> cpm radioactive probe in prehybridization buffer at 50°C overnight. After rinsing 3  $\times$  5 min in 4 $\times$  SSC (20 $\times$  SSC: 1% (w/v) BSA, 1% (w/v) Ficoll-400, 1% (w/v) polyvinylpyrrolidone), brain slices were treated at 37°C (30 min) with RNase A and rinsed. For visualization, slides were dehydrated, covered with photo emulsion and exposed to radiographic film for 1 week at 4°C. Visualization of tissue structure was achieved with haematoxylin–eosin staining.

**Hybridization procedure for DIG-labelled probes.** DIG-labelled A<sub>1</sub> receptor RNA probes were synthesized by *in vitro* transcription (DIG-dUTP RNA Labelling Kit, Roche Diagnostics, Mannheim, Germany) based on the vector above. Probes were purified with lithium chloride precipitation and subsequently tested for integrity and DIG labelling. Fixed brain slices on slides were acetylated in 100 mM triethanolamine and 2.5 ml l<sup>-1</sup> acetic anhydride in PBS for 10 min followed by dehydration with ethanol (50/70/95/99.8%) for 3 min each step. Subsequently, slides were covered with prehybridization buffer (62.5% formamide, 25% dextran sulfate, 7.5% NaCl (5000 mM), 2.5%, Denhardt's solution (50%), 1.25% Tris, 0.25% EDTA (500 mM)) at 58°C for 2 h in a humidity chamber. Hybridization was performed in prehybridization buffer to which was added 400 ng ml<sup>-1</sup> probe at 58°C in a humidity chamber overnight. Slices were treated with RNase A (37°C, 30 min) and unspecific binding was blocked in 2 $\times$  SSC, 0.05% Triton X-100 and 2% normal goat serum (NGS); they were incubated with horseradish peroxidase-linked anti-DIG antibody (37°C, 2 h) and visualized with 50 mg ml<sup>-1</sup> 5-bromo-4-chloro-3'-indolyphosphate p-toluidine and 70 mg ml<sup>-1</sup> nitro-blue tetrazolium chloride overnight. Images were acquired with a bright field microscope (BX51, Olympus, Hamburg, Germany). Images of *in situ* hybridization using wild-type tissue and sense probes as well as A1 knockout tissue and antisense probes served as control. These images were contrast-enhanced by adjusting histogram levels (white level set to 240, gamma set to 0.67; Photoshop CS6, Adobe, San Jose, CA, USA) to improve visibility of the tissue outline.

### Data analysis and statistics

Patch-clamp recordings were analysed using Mini Analysis (Synaptosoft, Fort Lee, NJ, USA), ClampFit (Molecular Devices, Biberach, Germany) and OriginPro (OriginLab Corp., Northampton, MA, USA). Membrane potential values recorded in current clamp using a low-chloride pipette solution were corrected for a liquid junction potential of  $-18$  mV. All values are means  $\pm$  standard

error of the mean (SEM) with  $n$  representing the number of analysed cells. Statistical analysis was performed using one-way ANOVA with Fisher's *post hoc* test or Student's *t* test. Means were defined as statistically different at error probabilities  $P < 0.05$  (\*),  $P < 0.01$  (\*\*) and  $P < 0.001$  (\*\*\*)).

## Results

### Adenosine A<sub>1</sub> receptor gene expression in olfactory bulb mitral cells

We first assessed the expression profile of the A<sub>1</sub> adenosine receptor gene (*ADORA1*) in parasagittal sections of the mouse brain. As described before (Mahan *et al.* 1991; Reppert *et al.* 1991), we detected high levels of A<sub>1</sub> receptor mRNA in hippocampus and cerebellum. In addition, we found A<sub>1</sub> receptor expression in the olfactory bulb (Fig. 1A). One of the strongest expression signals of A<sub>1</sub> in the entire brain was found in the olfactory bulb mitral cell layer. At higher magnification, it became evident that the expression signal in the mitral cell layer correlated to large cell bodies of mitral cells (Fig. 1B and C). In the external plexiform layer and the basal part of the glomerular layer, cell bodies presumably reflecting tufted and external tufted cells were labelled. The expression of A<sub>1</sub> receptor gene, as assessed by *in situ* hybridization, was very low in the outer

part of the glomerular layer and the granule cell layer. A<sub>1</sub> adenosine receptor expression was not observed using the sense probe and in A<sub>1</sub> receptor knockout mice using the antisense probe, confirming the specificity of the *in situ* hybridization probes (Fig. 1D–G).

Expression of the A<sub>2A</sub> adenosine receptor gene (*ADORA2A*) was most prominent in the caudate putamen and the olfactory bulb (Dixon *et al.* 1996; Svenningsson *et al.* 1997; Kaelin-Lang *et al.* 1999). The expression of A<sub>2A</sub> in the olfactory bulb was more widespread compared to A<sub>1</sub> receptors and was detected in cells of all layers of the olfactory bulb, including mitral cells (Fig. 1H–J). Hence, high levels of adenosine receptor expression were found in the olfactory bulb and in particular in mitral cells, emphasizing the possible role of adenosine as a neuro-modulator in this brain area.

### Activation of adenosine A<sub>1</sub> receptors hyperpolarizes mitral cells

Physiological data suggest that adenosine might play a role in modulation of neuronal performance in the olfactory bulb (reviewed in Lohr *et al.* 2014). Therefore, we tested the effect of adenosine on the membrane potential of mitral cells. Mitral cells of wild-type mice had a mean resting membrane potential of  $-63.0 \pm 0.6$  mV ( $n = 23$ ),

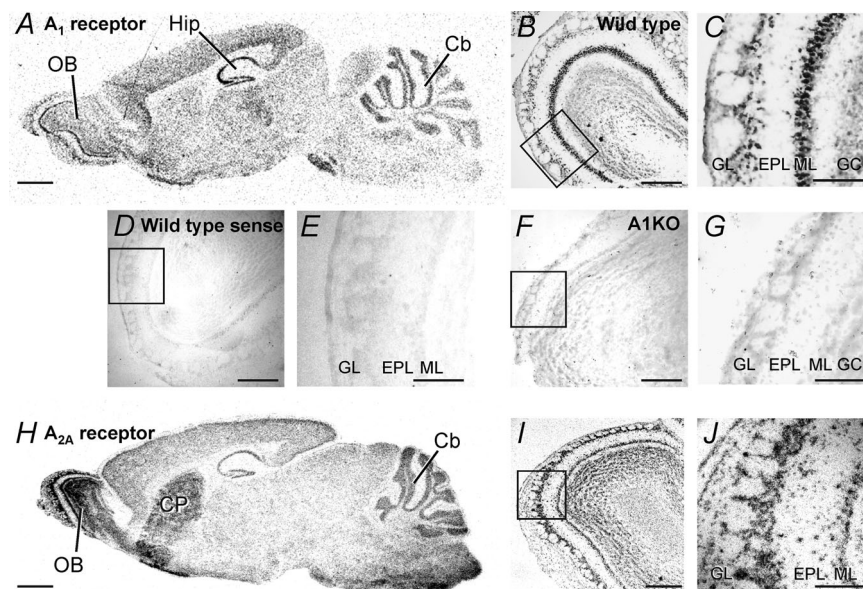


**Figure 1. Adenosine receptor gene expression**

A, *in situ* hybridization of A<sub>1</sub> receptor mRNA in mouse brain. Strong signals were detected in the olfactory bulb (OB), the hippocampus (Hip) and the cerebellum (Cb). B and C, the strongest A<sub>1</sub> receptor expression signal in the OB was located in large cells of the mitral cell layer (ML). D–G, no expression signal could be detected in wild-type mice using sense probes as a control (D and E), and in A<sub>1</sub> receptor knockout mice using the antisense probe (F and G). H, *in situ* hybridization of A<sub>2A</sub> receptor mRNA. A<sub>2A</sub> signals were detected in the olfactory bulb, the cerebellum and the caudate putamen (CP). I and J, significant A<sub>2A</sub> expression was localized in all layers of the OB. EPL, external plexiform layer; GCL, granule cell layer; GL, glomerular layer. Scale bars: 1 mm in A and H; 300  $\mu$ m in B, D, F and I; 100  $\mu$ m in C, E, G and J.

which hyperpolarized by  $2.6 \pm 0.4$  mV ( $n = 35$ ) upon application of  $100 \mu\text{M}$  adenosine for 30 s (Fig. 2A, left panel). The membrane potential recovered slowly to resting values, presumably due to the slow bath perfusion kinetics. In addition, we cannot exclude the involvement of a sustained component in the adenosine-stimulated signalling pathway leading to hyperpolarization. In  $A_1$  receptor knockout mice, mitral cells did not hyperpolarize due to adenosine application, but instead depolarized by  $0.4 \pm 0.2$  mV ( $n = 9$ ,  $P = 0.005$ ), suggesting that  $A_1$  receptors mediate the adenosine-evoked hyperpolarization (Fig. 2A, right panel). The hyperpolarizing effect of adenosine in wild-type mice was mimicked by application of the  $A_1$  agonist  $N^6$ -CPA (Fig. 2B).  $1 \mu\text{M}$  of  $N^6$ -CPA evoked a hyperpolarization of  $2.8 \pm 0.4$  mV ( $n = 13$ ). In the presence of the potent and selective  $A_1$  receptor antagonist DPCPX ( $1 \mu\text{M}$ ), no change in membrane potential was evoked by adenosine ( $n = 6$ ),

confirming that adenosine hyperpolarized mitral cells by activation of  $A_1$  receptors (Fig. 2C). DPCPX alone had no effect on the resting membrane potential and the resting firing rate of mitral cells. The pharmacological profile of the adenosine-mediated effect on mitral cells, summarized in Fig. 2D, clearly demonstrates an activation of  $A_1$  receptors by adenosine. Previous studies demonstrated release of ATP from olfactory sensory neurons and its degradation to adenosine in glomeruli (Doengi *et al.* 2008; Thyssen *et al.* 2010), leading to the hypothesis that the adenosine-mediated hyperpolarization in mitral cells mainly originates from the apical tuft in the glomerulus. Therefore, we compared the hyperpolarization evoked by adenosine between mitral cells with intact apical dendrite and mitral cells in which the apical tuft had been cut during preparation of brain slices, as visualized by the fluorescent tracer Alexa Fluor 594 added to the pipette solution. We did not find a significant difference in

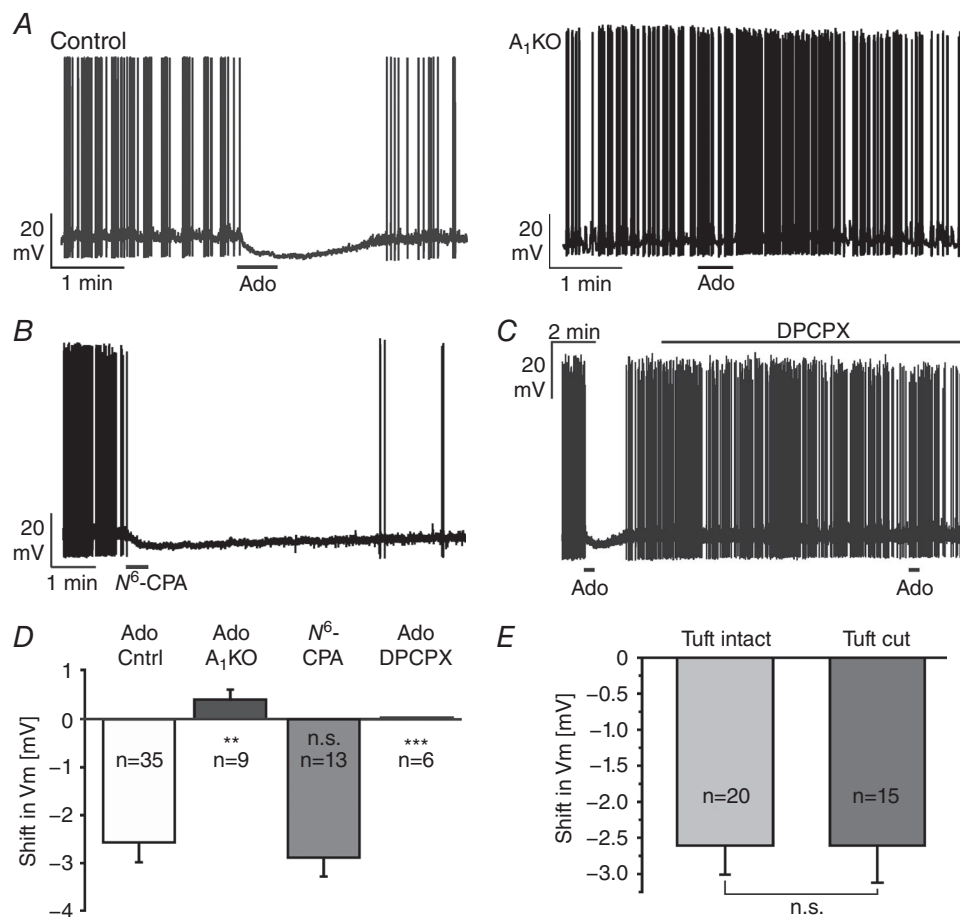


**Figure 2. Adenosine hyperpolarizes mitral cells by  $A_1$  receptor activation**

*A*,  $100 \mu\text{M}$  adenosine (Ado) leads to a hyperpolarization of mitral cells in wild-type (control) but not in  $A_1$  knockout mice ( $A_1$ KO). *B*, the  $A_1$  receptor agonist  $N^6$ -CPA ( $1 \mu\text{M}$ ) mimics the effect of adenosine. *C*, the  $A_1$ -selective antagonist DPCPX ( $1 \mu\text{M}$ ) inhibited the adenosine-evoked hyperpolarization. *D*, summary of the pharmacological investigation of the adenosine-induced membrane potential shift. n.s., not significant. *E*, no significant difference (n.s.) in the adenosine-evoked hyperpolarization was found between mitral cells with intact apical dendrite and mitral cells with cut apical dendrite.

the adenosine-evoked hyperpolarization between these groups (Fig. 2E). Adenosine evoked a hyperpolarization of  $2.6 \pm 0.4$  mV ( $n = 20$ ) in intact mitral cells and  $2.6 \pm 0.7$  mV ( $n = 15$ ) in mitral cells with cut apical tuft, indicating that the adenosine-evoked hyperpolarization does not mainly derive from the apical tuft.

### A<sub>1</sub> receptor activation increases the membrane conductance in mitral cells

The adenosine-evoked hyperpolarization via A<sub>1</sub> receptors could be caused either by the closure of depolarizing non-specific cation channels or by an opening of hyperpolarizing Cl<sup>-</sup> or K<sup>+</sup> channels. To assess whether channels are opened or closed by application of adenosine, we measured the membrane conductance in voltage-clamped mitral cells (holding potential: -70 mV) in the presence of the glutamate receptor antagonists NBQX (10 μM) and D-APV (50 μM), the GABA<sub>A</sub> receptor antagonist gabazine (10 μM) and TTX (1 μM) to synaptically isolate the recorded mitral cell from its neuronal network. Membrane conductance was assessed by applying voltage steps of -10 mV amplitude. Application of adenosine led to an outward current (Fig. 3A) and an increase in membrane conductance (Fig. 3B). Interestingly, the increase in membrane conductance outlasted the outward current and did not reach baseline within 5 min after washout of adenosine (Fig. 3C). On average, the membrane conductance significantly increased by  $21.4 \pm 4.4\%$  from

$3.24 \pm 0.8$  to  $3.55 \pm 0.8$  nS ( $n = 6$ ;  $P < 0.001$ ) upon application of adenosine, indicating that A<sub>1</sub> receptors in mitral cells are linked to the opening of ion channels that mediate hyperpolarization such as Cl<sup>-</sup> or K<sup>+</sup> channels.

We tested the involvement of Cl<sup>-</sup> channels by using a modified pipette solution in order to shift the reversal potential for Cl<sup>-</sup>. The calculated Cl<sup>-</sup> reversal potential using the standard (low Cl<sup>-</sup>) pipette solution was -61 mV, which is close to the resting membrane potential. We used a high Cl<sup>-</sup> pipette solution resulting in a calculated Cl<sup>-</sup> reversal potential of -16 mV. Hence, under the latter conditions, opening of Cl<sup>-</sup> channels should have led to depolarization. However, application of adenosine elicited a hyperpolarization, regardless of which pipette solution was used (Fig. 3D). The amplitudes of the hyperpolarizations measured with different pipette solutions were not significantly different, suggesting that Cl<sup>-</sup> channels make no major contribution to the adenosine-mediated hyperpolarization (Fig. 3E).

### A<sub>1</sub> receptors activate K<sup>+</sup> channels

We determined the reversal potential of the adenosine-mediated membrane potential shift in current-clamp by stepping to different membrane potentials using the standard pipette solution and defined current steps (50 pA interval) in the absence and in the presence of adenosine (Fig. 4A). We used a combination of K<sup>+</sup> concentrations in the extracellular (5 mM) and pipette

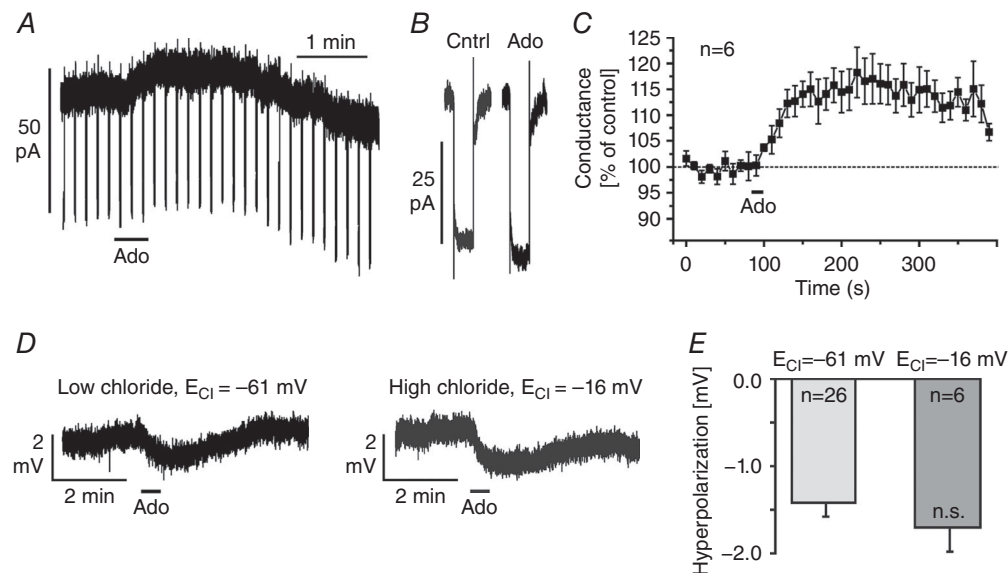


**Figure 3. Adenosine increases the membrane conductance**

A, membrane conductance was measured by hyperpolarizing voltage steps of -10 mV in presence of TTX (1 μM), NBQX (10 μM), D-APV (50 μM) and gabazine (10 μM). B and C, application of 100 μM adenosine increased the membrane conductance. D, adenosine-induced hyperpolarization as measured in whole-cell current-clamp configuration using pipette solutions with different chloride concentrations, resulting in calculated chloride reversal potentials ( $E_{Cl}$ ) of -61 and -16 mV, respectively. E, the adenosine-evoked hyperpolarization was independent of the chloride reversal potential (n.s., not significant).

solution (140 mM) that resulted in a calculated  $K^+$  reversal potential of  $-86$  mV. On average, at membrane potentials more positive than  $-90$  mV, adenosine tended to hyperpolarize the membrane, whereas at membrane potentials more negative than  $-90$  mV, adenosine depolarized the membrane (Fig. 4B). The reversal potential of

the adenosine-mediated shift in membrane potential as extrapolated from all recordings ( $n = 5$  cells) was  $-90$  mV, close to the calculated  $K^+$  reversal potential.

To confirm that adenosine activates a  $K^+$  conductance, we measured the ionic current evoked by adenosine in voltage-clamp experiments at different holding potentials.

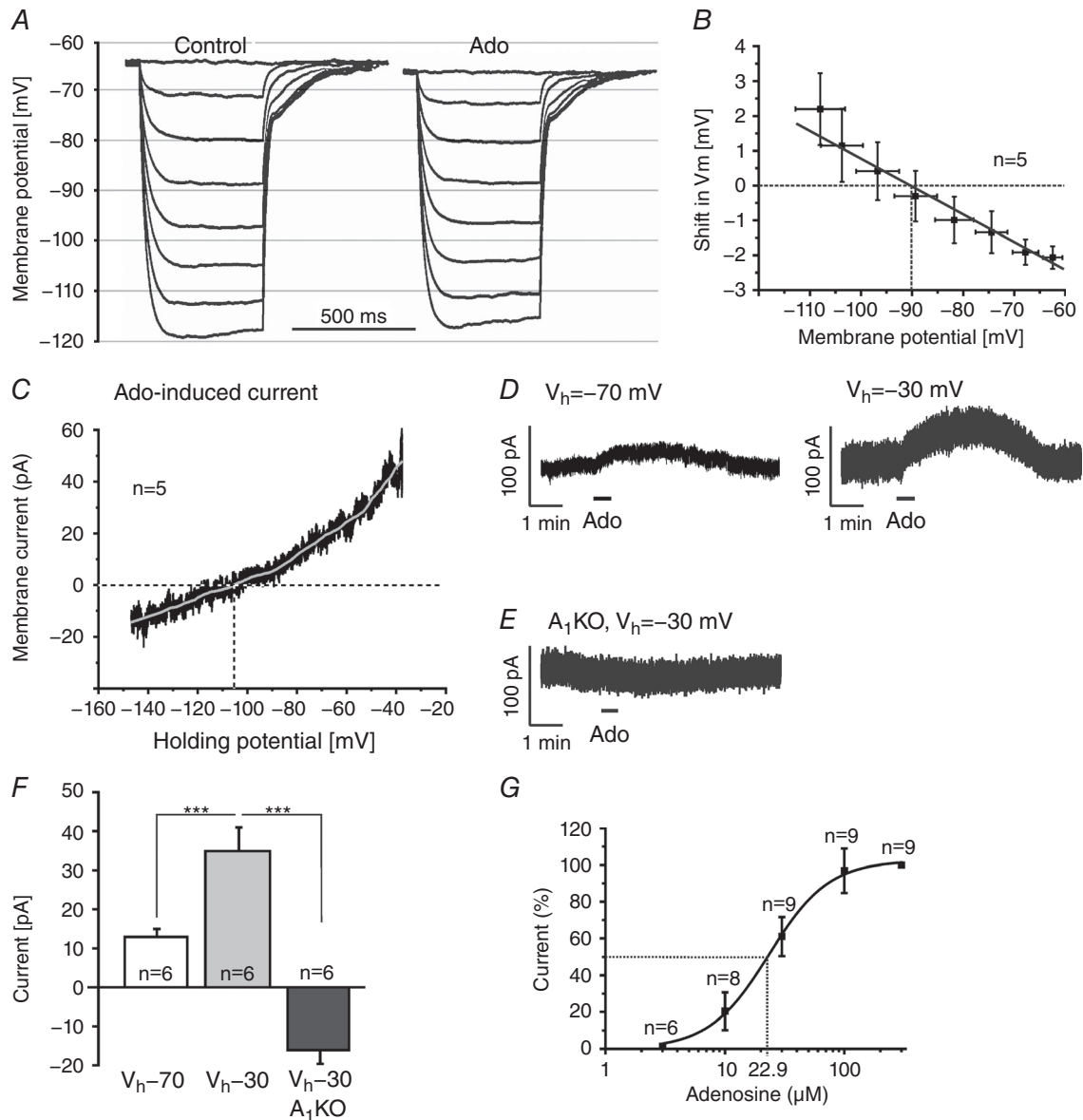


**Figure 4. Adenosine activates potassium channels**

**A**, shifts in membrane potential evoked by negative current injections ( $-50$  to  $-350$  pA) before (control) and in the presence of adenosine ( $100 \mu M$ ). **B**, extrapolation of adenosine-evoked membrane potential shifts at different baseline potentials (as measured during the current steps in control) revealed an average reversal potential of  $-90$  mV. **C**, current–voltage relationship of the adenosine-evoked current, averaged over recordings from five cells (black trace) and filtered (grey trace; Savitsky-Golay with second order polynomial and window size of 1501, corresponding to  $\pm 5$  mV), revealed a reversal potential of  $-106$  mV. **D**, outward current evoked by  $100 \mu M$  adenosine at a holding potential ( $V_h$ ) of  $-70$  mV and  $-30$  mV. **E**, adenosine failed to evoke outward currents in  $A_1$  receptor knockout mice. **F**, the adenosine-evoked outward current was significantly larger at  $V_h$  of  $-30$  mV compared to  $-70$  mV. At  $-30$  mV, adenosine evoked an inward current in  $A_1$  knockout mice. **G**, dose–response relationship of the adenosine-evoked outward current.



In these experiments the  $K^+$  reversal potential was set to  $-108$  mV to increase the driving force for  $K^+$  and, hence, the size of the responses evoked by adenosine. To assess the current–voltage relationship, the membrane potential was first clamped to  $-20$  mV for several minutes to inactivate voltage-dependent currents, followed by a voltage ramp from  $-20$  to  $-130$  mV within 800 ms. Voltage ramps were performed before and during application of  $100 \mu\text{M}$  adenosine, the difference revealing the adenosine-evoked current. After correction for the liquid junction potential of  $-18$  mV, this resulted in an adenosine-evoked outwardly rectifying current that reversed at  $-106$  mV and continued as inward current at more negative membrane potentials ( $n = 5$ ; Fig. 4C). To quantify the effect of the membrane potential on the outward current, we measured adenosine-induced currents at two holding potentials,  $-70$  and  $-30$  mV (Fig. 4D and G). At a holding potential of  $-70$  mV, adenosine evoked an outward current of  $13 \pm 2$  pA ( $n = 6$ ; Fig. 4D, left panel). The outward current significantly increased to  $35 \pm 6$  pA ( $n = 6$ ,  $P < 0.001$ ) at a holding potential of  $-30$  mV (Fig. 4D, right panel). In  $A_1$  knockout mice, adenosine failed to induce membrane currents (Fig. 4E) or resulted in inward currents instead of outward currents, verifying the involvement of  $A_1$  receptors. On average, the adenosine-mediated effect amounted to  $-16 \pm 4$  pA ( $n = 6$ ,  $P < 0.001$  as compared to wild-type) in  $A_1$  knockout mice (Fig. 4E and F). To achieve a dose–response curve for the adenosine-evoked response in wild-type mice, we tested adenosine concentrations ranging from 3 to  $300 \mu\text{M}$  and measured the evoked outward currents ( $n = 9$ ). The results revealed an  $EC_{50}$  value of  $22.9 \mu\text{M}$  (Fig. 4G). In summary, these experiments indicate that the adenosine-mediated current is caused by an  $A_1$  receptor-activated potassium conductance.

### Pharmacological characterization of the adenosine-activated $K^+$ conductance

Activation of GIRK mediated by  $A_1$  receptors is a common pathway of adenosinergic neuromodulation (Sickmann & Alzheimer, 2003; Kim & Johnston, 2015). To test the involvement of GIRK in the adenosine-evoked hyperpolarization of olfactory bulb mitral cells, we applied adenosine in the presence of the GIRK inhibitor  $Ba^{2+}$  in current-clamp experiments using TTX to suppress neuronal activity.  $Ba^{2+}$  at  $1$  mM, a concentration sufficient to block GIRK (Sickmann & Alzheimer, 2003; Kim & Johnston, 2015), resulted in depolarization of the membrane of mitral cells and an increase in the frequency of synaptic miniature potentials, which largely recovered following washout of adenosine (Fig. 5A). However,  $Ba^{2+}$  had no inhibiting effect on the adenosine-induced hyperpolarization ( $n = 6$ ). In addition, we used canonical blockers of voltage-gated  $K^+$  channels at concentrations

demonstrated to efficiently and selectively block  $K^+$  channel subtypes (Gutman *et al.* 2005; Wei *et al.* 2005). 4-AP ( $10$  mM;  $n = 7$ ) and TEA ( $10$  mM;  $n = 5$ ) did not significantly reduce adenosine-evoked hyperpolarizations (Fig. 5B and C). To reveal the type of  $K^+$  channel involved, we additionally tested five inhibitors for different  $K^+$  channel subfamilies for their effect on the adenosine-evoked hyperpolarization (Fig. 5D and E). Only bupivacaine significantly reduced the hyperpolarization. On average, bupivacaine reduced the adenosine-evoked hyperpolarization by  $41.3 \pm 9.0\%$  ( $n = 7$ ,  $P = 0.040$ ).

### $A_1$ receptors activate two-pore domain $K^+$ channels

Bupivacaine has been shown to inhibit some of the K2P channels, a large family of background  $K^+$  channels (Enyedi & Czirjak, 2010; Feliciangeli *et al.* 2015). To confirm the potential involvement of K2P channels we tested halothane, which activates some of the K2P channels, but inhibits other K2P channels such as bupivacaine-sensitive THIK channels (Patel *et al.* 2001; Rajan *et al.* 2001; Bushell *et al.* 2002). In voltage-clamp experiments ( $V_h -30$  mV),  $3$  mM halothane evoked a large inward current superimposed by a smaller outward current (Fig. 6A), demonstrating that a large part of the background current in mitral cells is carried by K2P channels. The halothane-evoked inward current presumably is the result of inhibition of halothane-inhibited K2P channels such as THIK-1, while the small outward current may reflect halothane-activated K2P channels such as TREK and TASK (Enyedi & Czirjak, 2010; Feliciangeli *et al.* 2015). In the presence of halothane, the adenosine-evoked outward current was significantly inhibited by  $33.7 \pm 10.4\%$  ( $n = 7$ ,  $P = 0.043$ ; Fig. 6B). In addition, bupivacaine reduced the adenosine-induced outward current by  $69.9 \pm 8.6\%$  ( $n = 6$ ,  $P < 0.001$ ; Fig. 6C). The effect of bupivacaine was partly reversible after 10 min of washout of bupivacaine. The results indicate that  $A_1$  receptors modulate a bupivacaine-sensitive and halothane-sensitive background  $K^+$  conductance (Fig. 6D).

### $A_1$ receptors fail to modulate synaptic input from sensory axons

Mitral cells receive synaptic input from olfactory sensory neurons. Synaptic transmission between axons of sensory neurons and mitral cells is subject to extensive neuromodulation by GABA and dopamine (Aroniadou-Anderjaska *et al.* 2000; Ennis *et al.* 2001; Maher & Westbrook, 2008). We were interested in whether adenosine was also capable of modulating synaptic input from olfactory sensory neurons in mitral cells. We measured synaptic currents in mitral cells in response to single pulse stimulation of sensory axons (Fig. 7A).

On average, the amplitude of synaptic currents upon axonal stimulation was  $-130.7 \pm 32.7$  pA ( $n = 6$ ) and was not affected by application of adenosine (Fig. 7B). As a measure of synaptic vesicle fusion in terminals of olfactory sensory axons, we employed a mouse strain in which olfactory sensory neurons express the vesicle fusion marker syn-pH (Fig. 7C). Changes in syn-pH fluorescence correlate linearly with the transmitter release in receptor axons (Bozza *et al.* 2004). Fluorescence transients evoked by stimulation of olfactory sensory axons were not reduced in amplitude by application of adenosine ( $n = 4$ ; Fig. 7D). The results indicate that the synaptic input from sensory neurons in mitral cells is not influenced by adenosine.

### A<sub>1</sub> receptors improve the signal-to-noise ratio of mitral cell output signals

Odour information derived from olfactory sensory neurons is processed in the olfactory bulb and propagated by mitral and tufted cells into higher brain centres such as the piriform cortex. The relationship between sensory input signals and mitral cell output signals is one

important determinant of odour perception. To assess whether the output signal of mitral cells resulting from sensory stimulation is affected by adenosine, we recorded action currents in the cell-attached configuration, hence avoiding dialysis of the recorded cell that could compromise excitability. Single stimulation of sensory axons resulted in a biphasic increase in firing rate of the mitral cell (Fig. 8A). This biphasic increase in firing rate consisted of an early response of approximately 100 ms duration, followed by a late response of approximately 400 ms after a short gap devoid of action potential firing (Fig. 8A, right panel). The averaged firing rate increased from  $5.2 \pm 1.6$  Hz at baseline (averaged from 19 s preceding the stimulation) to  $29.1 \pm 6.0$  Hz ( $P < 0.001$ ) during the early response phase (averaged from 0 to 100 ms after stimulation) and to  $10.9 \pm 3.1$  Hz ( $P < 0.001$ ) in the late response phase (averaged from 100 to 500 ms after stimulation) ( $n = 10$ ; Fig. 8B). The latency of the first action potential after stimulation was  $8.4 \pm 1.3$  ms ( $n = 10$ ) and displayed very little variance within a given experiment (Fig. 8C), suggesting that the early response resulted from monosynaptic transmission (De Saint Jan

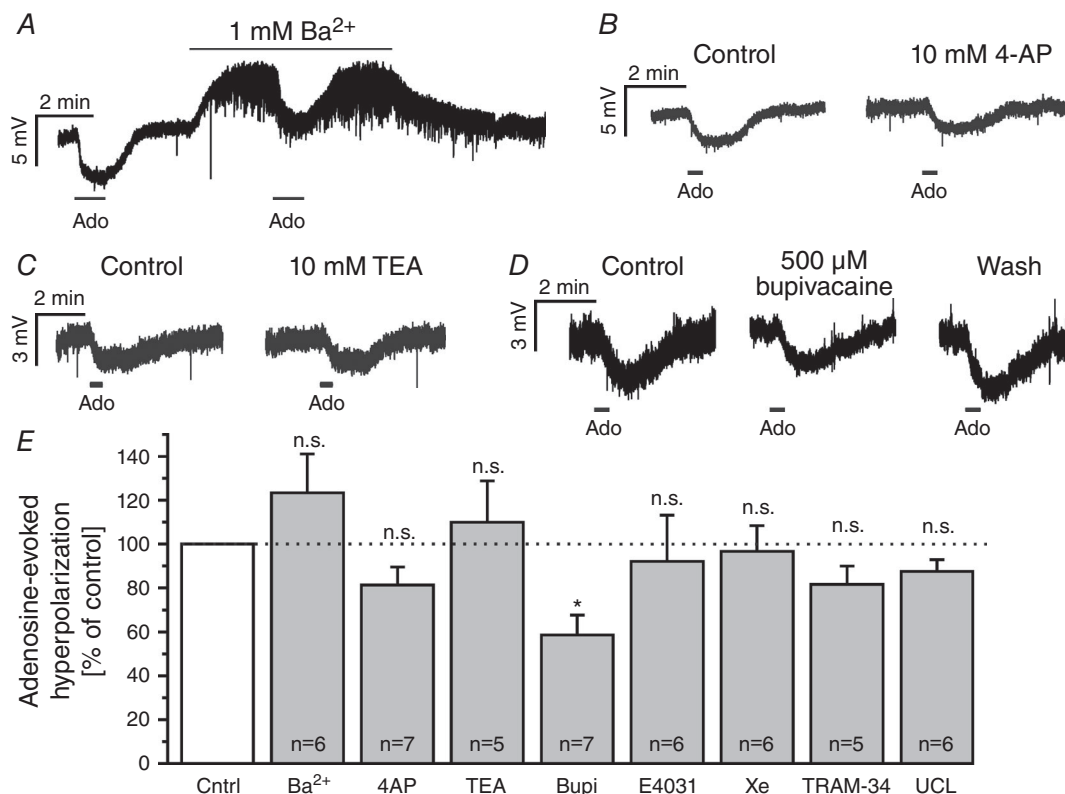


**Figure 5. Adenosine activates non-canonical potassium channels**

A–D, effect of 1 mM Ba<sup>2+</sup> (A), 10 mM 4-AP (B), 10 mM TEA (C) and 500 μM bupivacaine (D) on the adenosine-evoked hyperpolarization. E, effects of blockers of inwardly rectifying (1 mM Ba<sup>2+</sup>), canonical voltage-gated (10 mM 4-AP, 10 mM TEA), two-pore domain (500 μM bupivacaine), erg (10 μM E-4031), 'M'-current (20 μM XE 991) and calcium-activated (1 μM TRAM-34, 1 μM UCL 1684) potassium channels. Only bupivacaine significantly reduced the amplitude of adenosine-evoked hyperpolarization. All recordings were performed in the presence of 1 μM TTX. n.s., not significant.

*et al.* 2009) as opposed to disynaptic transmission found upon weak stimulation (Gire *et al.* 2012). The latency of the first action potential was not altered by adenosine, confirming lack of modulation of the synaptic input from sensory axons (Fig. 8D).

We next tested whether adenosine was able to affect the pattern of action potential firing evoked by electrical stimulation of olfactory sensory neurons (Fig. 9A). Adenosine reduced the baseline firing rate of mitral cells by  $37 \pm 6\%$  ( $n = 10$ ,  $P = 0.002$ ), while it had no significant effect on the firing rate in the presence of DPCPX ( $n = 6$ ) (Fig. 9B). Adenosine had no effect on the firing rate during the early response in both the absence and the presence of DPCPX, but decreased the firing rate of the late response in wild-type mice by  $36 \pm 5\%$  ( $n = 10$ ,  $P = 0.002$ ; Fig. 9C and D). As adenosine hyperpolarizes the mitral cell membrane by 2–3 mV, we examined whether this hyperpolarization was sufficient to cause the described effect of adenosine on stimulation-evoked action potential firing. Therefore, we hyperpolarized mitral cells in current-clamp mode by approximately 3 mV by current injection (–15 to –30 pA) and recorded action potentials evoked by single pulse stimulation of olfactory sensory neurons (Fig. 9E). In current-clamp recordings, baseline firing frequency was  $5.1 \pm 1.3$  Hz ( $n = 5$ ) and increased upon single pulse stimulation to  $40.0 \pm 6.7$  Hz ( $n = 5$ ) during the early response and to  $16.5 \pm 2.0$  Hz ( $n = 5$ )

during the late response. The induced hyperpolarization decreased the baseline firing rate by  $61 \pm 5\%$  ( $n = 5$ ,  $P = 0.038$ ) and the late response firing rate by  $38 \pm 6\%$  ( $n = 5$ ,  $P = 0.018$ ), but had no effect on the early response (Fig. 9F–H). Since spontaneous firing reflects the mitral cell output activity independent of specific odour sensation it can be considered as noise, whereas the early response reflects the signal directly evoked by sensory input and propagated to the cortex upon odour sensation as mimicked by stimulation of sensory axons. Hence, the ratio of early response/spontaneous firing is an estimation of the signal-to-noise ratio of the mitral cell output. The signal-to-noise ratio of  $8.4 \pm 1.9$  under control conditions increased significantly by  $62 \pm 23\%$  ( $n = 10$ ,  $P = 0.045$ ) upon application of adenosine in the absence but not in the presence of DPCPX (not shown). In addition, the signal-to-noise ratio increased by  $164 \pm 50\%$  ( $n = 5$ ,  $P = 0.002$ ) upon current-induced hyperpolarization (Fig. 9I). We also calculated the signal-to-noise ratio of the late response. Since both baseline firing and firing during the late response were reduced by adenosine, the ratio of late response/baseline was not altered by adenosine

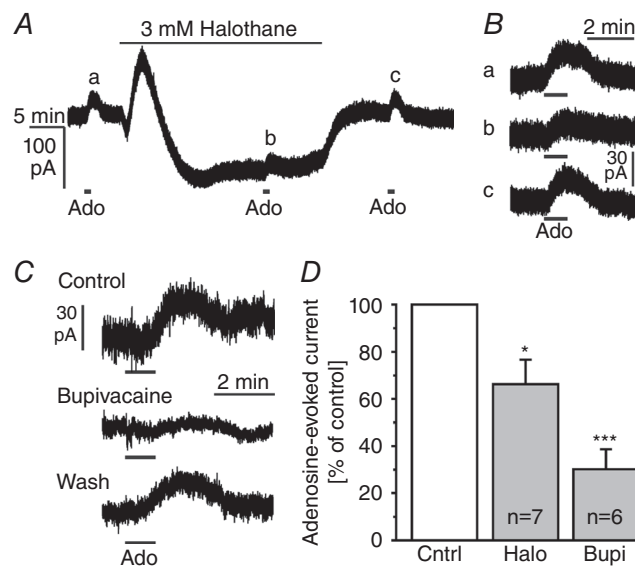


**Figure 6. Adenosine activates two-pore domain-like potassium channels**

A, effect of the two-pore domain  $K^+$  channel ligand halothane on the membrane current. B, effect of halothane on outward currents evoked by adenosine ( $100 \mu\text{M}$ ), as measured at the time points a–c indicated in A. C, effect of bupivacaine on the outward current evoked by adenosine ( $100 \mu\text{M}$ ). D, halothane and bupivacaine significantly reduced the adenosine-evoked outward currents.

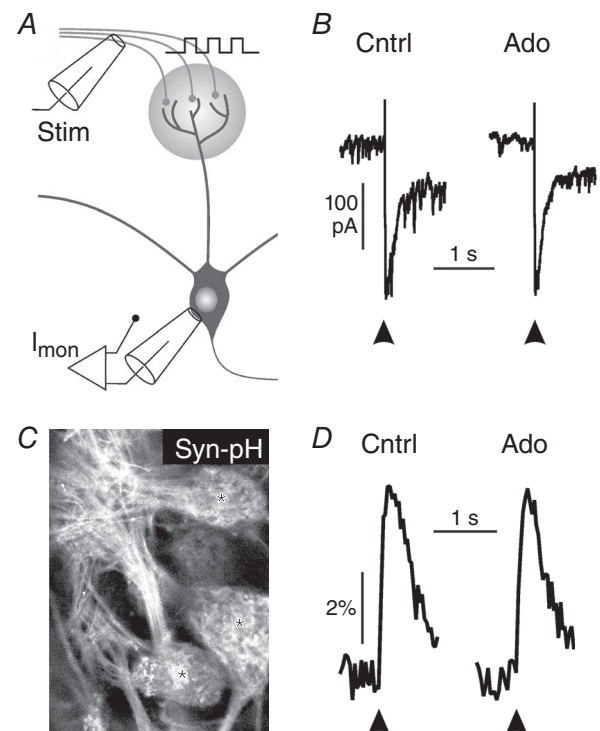


**Figure 7. Adenosine has no effect on synaptic input from olfactory sensory neurons**

A, schematic drawing of the experimental set-up. Stim, stimulation;  $I_{\text{mon}}$ , current monitor. B, mitral cell synaptic currents evoked by single pulse stimulation of sensory axons in the absence and presence of adenosine ( $100 \mu\text{M}$ ). C, expression of synapto-pHluorin in olfactory sensory axons. D, adenosine ( $100 \mu\text{M}$ ) did not alter stimulation-induced synapto-pHluorin fluorescence transients.

(Fig. 9I). However, it increased upon current-induced hyperpolarization by  $71 \pm 27\%$  ( $n = 5$ ;  $P = 0.049$ ). The results indicate that  $A_1$  receptor activation is able to increase the signal-to-noise ratio particularly of the firing pattern directly evoked in mitral cells upon synaptic input from sensory neurons and hence to modulate olfactory information that is propagated from the olfactory bulb to other brain areas such as the piriform cortex.

## Discussion

The olfactory bulb is a brain region with one of the highest activities of enzymes involved in extracellular ATP degradation and adenosine production (Langer *et al.* 2008), suggesting an important role of adenosinergic neuromodulation in this sensory pathway. In the present study, we investigated the effect of adenosine on mitral cell membrane properties in the olfactory bulb. Adenosine increased the background  $K^+$  conductance

by activation of  $K_2P$  channels, a modulatory pathway not described in neurons before. The increased  $K^+$  conductance reduced spontaneous action potential firing (noise), but had no effect on synaptic input in mitral cells derived from olfactory sensory neurons and the subsequent bursting in mitral cells (signal), resulting in an improved signal-to-noise ratio.

## Adenosine modulates potassium channels

Based on membrane conductance measurements and calculation of the reversal potential of the adenosine-induced ion conductance, we showed that  $A_1$  receptor activation leads to opening of background potassium channels. Our pharmacological data suggest the involvement of  $K_2P$  channels, which are sensitive to volatile anaesthetics such as chloroform, isoflurane and halothane (Enyedi & Czirjak, 2010; Feliciangeli *et al.* 2015). Halothane induced a large inward current, suggesting

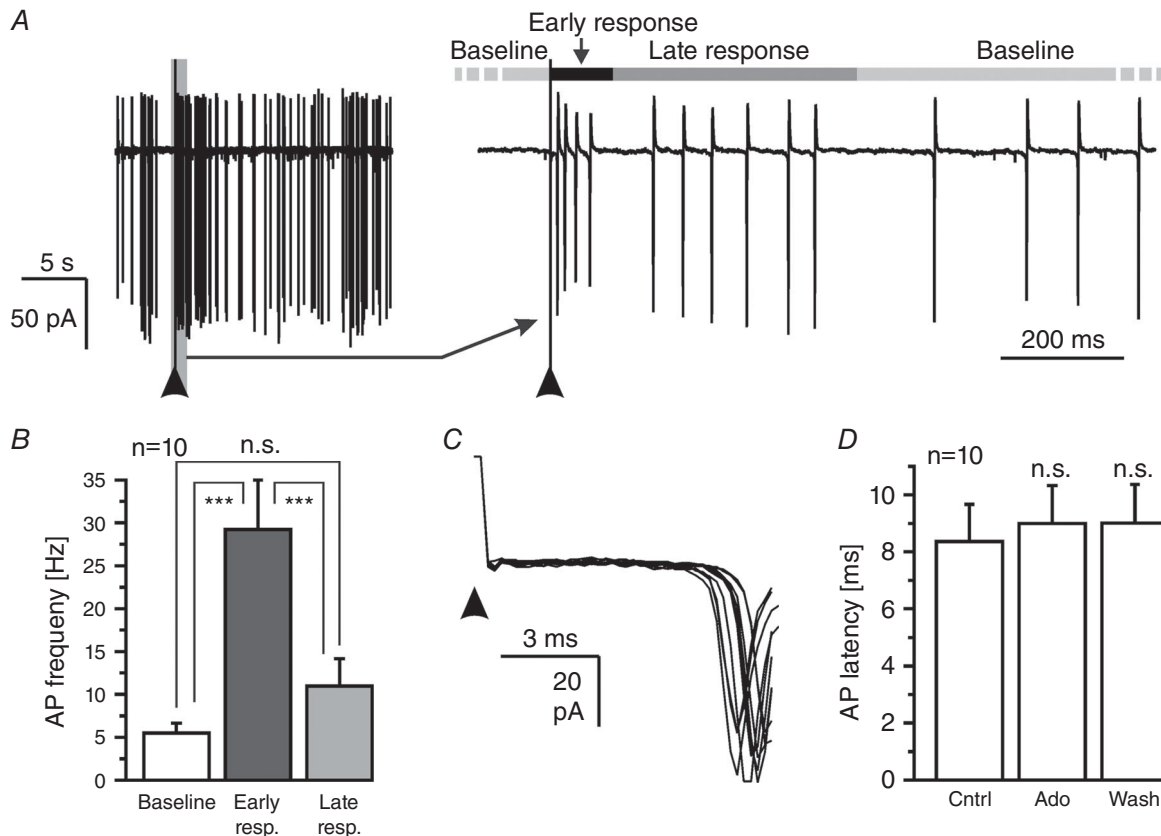


**Figure 8. Synaptic input from olfactory sensory neurons evokes a complex pattern of action potential firing**

A, mitral cell response (recorded in cell-attached configuration) upon single pulse stimulation of axons of olfactory sensory neurons ( $100 \mu A$ ,  $50 \mu s$ ; indicated by an arrowhead). The response was divided into an early (0–100 ms) and a late response (100–500 ms). B, analysis of the spontaneous firing frequency and the firing frequency during early and late responses. C, 10 consecutive traces (20 s interval) of action current recordings following olfactory sensory axon stimulation measured in the same cell were superimposed to demonstrate little variance in latency. D, the latency between stimulation onset and AP firing was not affected by adenosine ( $100 \mu M$ ). n.s., not significant.

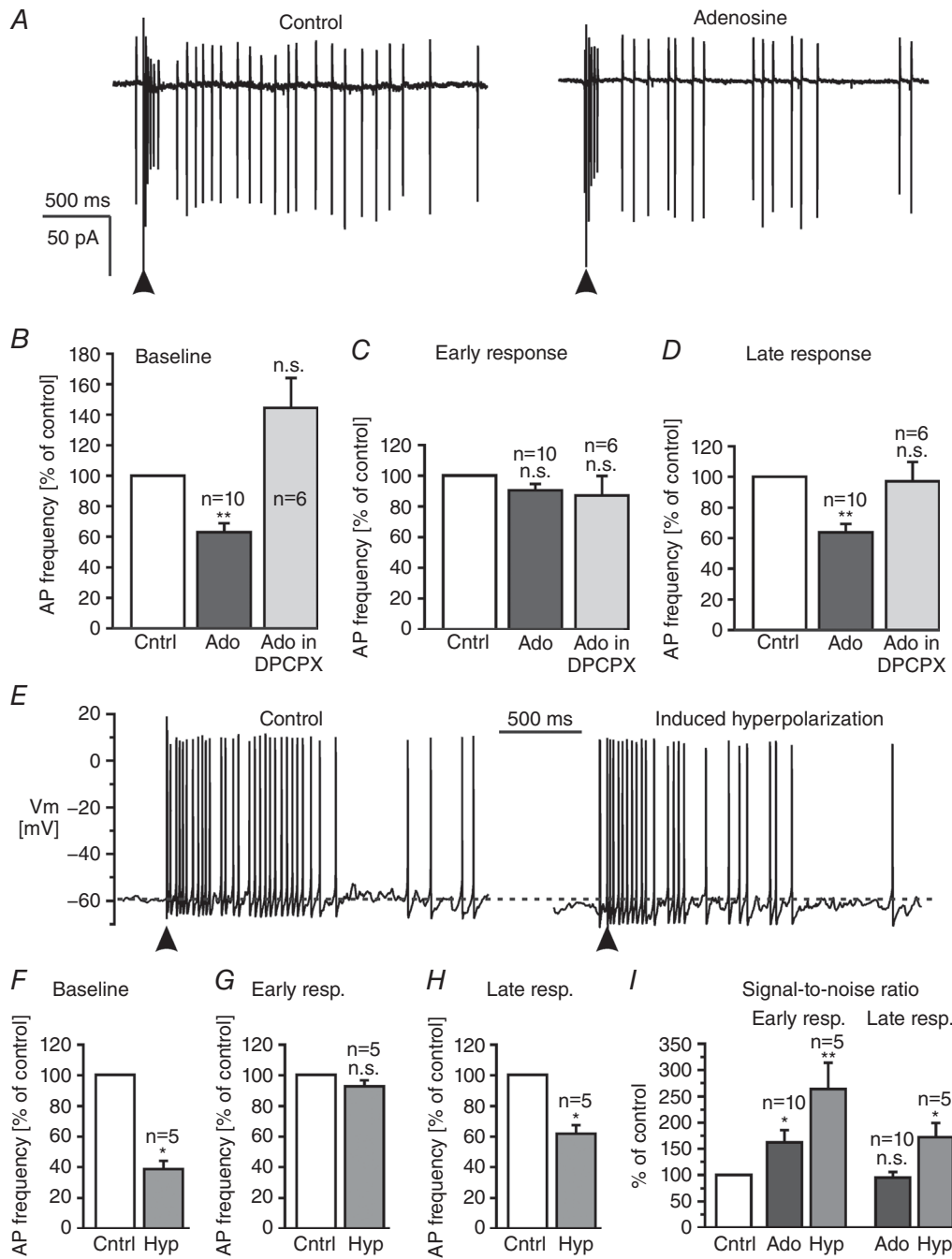


**Figure 9. Adenosine increases the signal-to-noise ratio of the input–output relationship of mitral cells** A, cell-attached recording of action potentials following single pulse stimulation ( $100 \mu\text{A}$ ,  $50 \mu\text{s}$ ; indicated by an arrowhead) of olfactory sensory neurons in the absence (control) and in the presence of  $100 \mu\text{M}$  adenosine. B, effect of adenosine on baseline firing, C and D, early response (C) and late response (D) in control experiments and in the presence of DPCPX. E, effect of hyperpolarization of approximately 3 mV induced by negative current injection on action potential firing evoked by electrical stimulation of olfactory sensory neurons in current clamp recordings. F, hyperpolarization (Hyp) significantly reduced the frequency of baseline firing, while G, firing rate of the early response was not affected. H, hyperpolarization reduced the firing rate of the late response. I, adenosine and current-induced hyperpolarization increased the signal-to-noise ratio of the early response in mitral cells. Adenosine had no effect on the signal-to-noise ratio of the late response, while induced hyperpolarization also increased the signal-to-noise ratio of the late response. n.s., not significant.

inhibition of K2P channels such as THIK-1 and THIK-2, which are highly expressed in the olfactory bulb, including mitral cells (Rajan *et al.* 2001; Lein *et al.* 2007), and can form heterodimers (Blin *et al.* 2014). The halothane-evoked inward current was superimposed by an outward current, suggesting that in addition to halothane-inhibited K2P channels, halothane-activated K2P channels are present in mitral cells, as shown before, for instance, in thalamic neurons (Meuth *et al.* 2003). Bupivacaine inhibits THIK-1 (Kang *et al.* 2014); however, the pharmacology of K2P channels is still poorly understood and the action of bupivacaine alone does not allow for a definite identification of the K2P channel activated by adenosine (Lesage, 2003). For instance, in our experiments barium did not block the adenosine-evoked hyperpolarization, while in Purkinje neurons a THIK-1-like current was reduced by barium (Bushell *et al.* 2002). Absent barium sensitivity clearly argues against the involvement of GIRK channels, which have been shown to mediate adenosine-induced hyperpolarization in other types of neurons and are activated by the  $\beta\gamma$  subunit of G-proteins coupled to  $A_1$  receptors and other metabotropic receptors (Lüscher & Slesinger, 2010). Several other types of potassium channels have been reported in mitral cells including SK channels, Shaker channels, erg channels and A-type channels (Fadool *et al.* 2004; Maher & Westbrook, 2005; Hirdes *et al.* 2009), but blockers of these channels did not affect the adenosine-mediated hyperpolarization. Modulation of K2P channels by intracellular signalling pathways in neuronal and non-neuronal cells has been published (Chen *et al.* 2006, Comoglio *et al.* 2014; Leist *et al.* 2017), but modulation of K2P channels by  $A_1$  receptors has been described only in retinal Müller glial cells so far (Skatchkov *et al.* 2006). In addition to  $A_1$  receptor expression, we found  $A_{2A}$  receptor expression in mitral cells. In  $A_1$  knockout mice, adenosine application resulted in slight depolarization instead of hyperpolarization, an effect that may be mediated by  $A_{2A}$  receptors, since  $A_{2A}$  receptors often exert opposing effects to  $A_1$  receptors (Cunha *et al.* 1994; Rebola *et al.* 2003).

### Adenosine modulates mitral cell activity

The pattern of action potentials propagated by mitral cells to cortical structures upon sensory stimulation is one of the main determinants of odour perception (Gire *et al.* 2013; Uchida *et al.* 2014). Synaptic input reaching mitral cells via olfactory sensory axons is not affected by adenosine, in contrast to other neuromodulators such as GABA (via  $GABA_B$  receptors) and dopamine which reduce neurotransmitter release at olfactory sensory axon terminals (Aroniadou-Anderjaska *et al.* 2000; Ennis *et al.* 2001; Maher & Westbrook, 2008). Firing of mitral cells evoked by synaptic input from olfactory sensory axons

comprises two phases, the early response reflecting direct excitation by the olfactory sensory afferents and the delayed response modulated by processing in the bulbar network (Najac *et al.* 2011). Timing of the early response with respect to the sniffing cycle may determine mitral cell response amplitudes (Smear *et al.* 2011); however, the latency of the early response to olfactory nerve stimulation is unaltered by adenosine, suggesting that adenosine does not impact temporal odour coding by early response modulation. In contrast, the frequency of spontaneous firing, but also of the firing in the late phase of the response, was reduced. The latter might result from  $A_1$  receptor-sensitive integration of feedback excitation and inhibition (Hayar *et al.* 2004; Giridhar *et al.* 2011; Gire *et al.* 2012; Carey *et al.* 2015; Liu *et al.* 2015; Parsa *et al.* 2015) and the results suggest that the temporal pattern of glomerular network activity is shaped by  $A_1$  receptors. Since the temporal pattern of glomerular network activity is decisive for odour perception (Shusterman *et al.* 2011; Haddad *et al.* 2013; Tripathy *et al.* 2013; Nunez-Parra *et al.* 2014; Uchida *et al.* 2014),  $A_1$  receptors might thus fine-tune odour perception. Recently it was reported that the input–output transformation in mitral and tufted cells contributes to the perception of odour concentration invariances (Storace & Cohen, 2017). Tuning of the input–output transformation by neuromodulators such as adenosine might therefore adjust the perception of odour concentration invariances. An increase in signal-to-noise ratio of the input–output transformation of mitral cells, comparable to the one described in the present study, has been found by stimulation of noradrenalin receptors in the olfactory bulb, which results in improved odour detection thresholds in behavioural tests (Escanilla *et al.* 2010; Manella *et al.* 2017). Adenosine increases the signal-to-noise ratio of the evoked firing pattern in mitral cells that are excited by the sensory stimulus; odour-evoked mitral cell responses, however, consist of a complex ensemble of both excited and inhibited mitral cells (Economo *et al.* 2016). In contrast to excitatory mitral cell responses, the signal-to-noise ratio of inhibitory responses would be attenuated by an adenosine-mediated reduction of spontaneous firing (noise), suggesting that the action of adenosine on information processing in the olfactory bulb might be even more complex than indicated by the present study. It must be noted that in awake animals, the response pattern of action potential firing upon sensory input, but also the spontaneous action potential firing of mitral cells, can differ from action potential firing in anaesthetized animals or slice preparations. Rinberg *et al.* (2006) reported an increased spontaneous firing rate of mitral cells in the awake situation compared to anaesthetized mice, while Kollo *et al.* (2014) found that about one-third of mitral cells were silent in awake mice, but not in anaesthetized mice. Since K2P channels are affected by anaesthetics such as

halothane and isoflurane used in some of the studies using anaesthetized animals, activation and/or inhibition of K2P channels in mitral cells by these anaesthetics may partly account for the differences between awake and anaesthetized mice.

Purinergic signalling has been described as affecting olfactory bulb neurons and glial cells via P2Y receptors and adenosine receptors, but the role of adenosine in odour information processing has not been elucidated before (Rieger *et al.* 2007; Doengi *et al.* 2008; Fischer *et al.* 2012; Roux *et al.* 2015). It should be noted that in the study by Roux *et al.* (2015) A<sub>1</sub> receptors appeared to increase excitability of mitral cells, whereas in our study activation of A<sub>1</sub> receptors reduced excitability, suggesting that adenosinergic modulation of mitral cell activity is intricate and variable.

In conclusion, our study shows that adenosine is able to modulate mitral cell membrane properties, attenuate network activity and tune the input–output relationship of mitral cell signalling. Hence, purinergic signalling might significantly contribute to odour information processing in the olfactory bulb.

## References

- Aroniadou-Anderjaska V, Zhou FM, Priest CA, Ennis M & Shipley MT (2000). Tonic and synaptically evoked presynaptic inhibition of sensory input to the rat olfactory bulb via GABA<sub>B</sub> heteroreceptors. *J Neurophysiol* **84**, 1194–1203.
- Blin S, Chatelain FC, Feliciangeli S, Kang D, Lesage F & Bichet D (2014). Tandem pore domain halothane-inhibited K<sup>+</sup> channel subunits THIK1 and THIK2 assemble and form active channels. *J Biol Chem* **289**, 28202–28212.
- Boison D (2009). Adenosine-based modulation of brain activity. *Curr Neuropharmacol* **7**, 158–159.
- Bozza T, McGann JP, Mombaerts P & Wachowiak M (2004). In vivo imaging of neuronal activity by targeted expression of a genetically encoded probe in the mouse. *Neuron* **42**, 9–21.
- Bushell T, Clarke C, Mathie A & Robertson B (2002). Pharmacological characterization of a non-inactivating outward current observed in mouse cerebellar Purkinje neurones. *Br J Pharmacol* **135**, 705–712.
- Carey RM, Sherwood WE, Shipley MT, Borisyuk A & Wachowiak M (2015). Role of intraglomerular circuits in shaping temporally structured responses to naturalistic inhalation-driven sensory input to the olfactory bulb. *J Neurophysiol* **113**, 3112–3129.
- Chen X, Talley EM, Patel N, Gomis A, McIntire WE, Dong B, Viana F, Garrison JC & Bayliss DA (2006). Inhibition of a background potassium channel by Gq protein  $\alpha$ -subunits. *Proc Natl Acad Sci USA* **103**, 3422–3427.
- Clark BD, Kurth-Nelson ZL & Newman EA (2009). Adenosine-evoked hyperpolarization of retinal ganglion cells is mediated by G-protein-coupled inwardly rectifying K<sup>+</sup> and small conductance Ca<sup>2+</sup>-activated K<sup>+</sup> channel activation. *J Neurosci* **29**, 11237–11245.
- Comoglio Y, Levitz J, Kienzler MA, Lesage F, Isacoff EY & Sandoz G (2014). Phospholipase D2 specifically regulates TREK potassium channels via direct interaction and local production of phosphatidic acid. *Proc Natl Acad Sci USA* **111**, 13547–13552.
- Cunha RA (2005). Neuroprotection by adenosine in the brain: From A<sub>1</sub> receptor activation to A<sub>2A</sub> receptor blockade. *Purinergic Signal* **1**, 111–134.
- Cunha RA, Johansson B, van der Ploeg I, Sebastião AM, Ribeiro JA & Fredholm BB (1994). Evidence for functionally important adenosine A<sub>2a</sub> receptors in the rat hippocampus. *Brain Res* **649**, 208–216.
- De Saint Jan D, Hirnet D, Westbrook GL & Charpak S (2009). External tufted cells drive the output of olfactory bulb glomeruli. *J Neurosci* **29**, 2043–2052.
- Dias RB, Rombo DM, Ribeiro JA, Henley JM & Sebastião AM (2013). Adenosine: setting the stage for plasticity. *Trends Neurosci* **36**, 248–257.
- Dixon AK, Gubitza AK, Sirinathsinghji DJ, Richardson PJ & Freeman TC (1996). Tissue distribution of adenosine receptor mRNAs in the rat. *Br J Pharmacol* **118**, 1461–1468.
- Doengi M, Deitmer JW & Lohr C (2008). New evidence for purinergic signaling in the olfactory bulb: A<sub>2A</sub> and P2Y<sub>1</sub> receptors mediate intracellular calcium release in astrocytes. *FASEB J* **22**, 2368–2378.
- Dos Santos-Rodrigues A, Pereira MR, Brito R, de Oliveira NA & Paes-de-Carvalho R (2015). Adenosine transporters and receptors: key elements for retinal function and neuroprotection. *Vitam Horm* **98**, 487–523.
- Economou MN, Hansen KR & Wachowiak M (2016). Control of mitral/tufted cell output by selective inhibition among olfactory bulb glomeruli. *Neuron* **20**, 397–411.
- Ennis M, Zhou F, Ciombor KJ, Aroniadou-Anderjaska V, Hayar A & Borrelli E (2001). Dopamine D2 receptor-mediated presynaptic inhibition of olfactory nerve terminals. *J Neurophysiol* **86**, 2986–2997.
- Enyedi P & Czirjak G (2010). Molecular background of leak K<sup>+</sup> currents: two-pore domain potassium channels. *Physiol Rev* **90**, 559–605.
- Escanilla O, Arrellanos A, Karnow A, Ennis M & Linstner C (2010). Noradrenergic modulation of behavioral odor detection and discrimination thresholds in the olfactory bulb. *Eur J Neurosci* **32**, 458–468.
- Fadool DA, Tucker K, Perkins R, Fasciani G, Thompson RN, Parsons AD, Overton JM, Koni PA, Flavell RA & Kaczmarek LK (2004). Kv1.3 channel gene-targeted deletion produces “Super-Smeller Mice” with altered glomeruli, interacting scaffolding proteins, and biophysics. *Neuron* **41**, 389–404.
- Feliciangeli S, Chatelain FC, Bichet D, Lesage F (2015). The family of K2P channels: salient structural and functional properties. *J Physiol* **593**, 2587–2603.
- Fischer T, Rotermund N, Lohr C & Hirnet D (2012). P2Y<sub>1</sub> receptor activation by photolysis of caged ATP enhances neuronal network activity in the developing olfactory bulb. *Purinergic Signal* **8**, 191–198.
- Fredholm BB, Chen JF, Cunha RA, Svenningsson P & Vaugeois JM (2005). Adenosine and brain function. *Int Rev Neurobiol* **63**, 191–270.

- Gire DH, Franks KM, Zak JD, Tanaka KF, Whitesell JD, Mulligan AA, Hen R & Schoppa NE (2012). Mitral cells in the olfactory bulb are mainly excited through a multistep signaling path. *J Neurosci* **32**, 2964–2975.
- Gire DH, Restrepo D, Sejnowski TJ, Greer C, De Carlos JA & Lopez-Mascaraque L (2013). Temporal processing in the olfactory system: can we see a smell? *Neuron* **78**, 416–432.
- Giridhar S, Doiron B & Urban NN (2011). Timescale-dependent shaping of correlation by olfactory bulb lateral inhibition. *Proc Natl Acad Sci USA* **108**, 5843–5848.
- Grundy D (2015). Principles and standards for reporting animal experiments in *The Journal of Physiology and Experimental Physiology*. *J Physiol* **593**, 2547–2549.
- Gundlfinger A, Bischofberger J, Jochenning FW, Torvinen M, Schmitz D & Breustedt J (2007). Adenosine modulates transmission at the hippocampal mossy fibre synapse via direct inhibition of presynaptic calcium channels. *J Physiol* **582**, 263–277.
- Gutman GA, Chandry KG, Grissmer S, Lazdunski M, McKinnon D, Pardo LA, Robertson GA, Rudy B, Sanguinetti MC, Stühmer W & Wang X (2005). International Union of Pharmacology. LIII. Nomenclature and molecular relationships of voltage-gated potassium channels. *Pharmacol Rev* **57**, 473–508.
- Haddad R, Lanjuin A, Madisen L, Zeng H, Murthy VN & Uchida N (2013). Olfactory cortical neurons read out a relative time code in the olfactory bulb. *Nat Neurosci* **16**, 949–957.
- Hayar A, Karnup S, Ennis M & Shipley MT (2004). External tufted cells: a major excitatory element that coordinates glomerular activity. *J Neurosci* **24**, 6676–6685.
- Hirdes W, Napp N, Wulfsen I, Schweizer M, Schwarz JR & Bauer CK (2009). Erg K<sup>+</sup> currents modulate excitability in mouse mitral/tufted neurons. *Pflugers Arch* **459**, 55–70.
- Housley GD, Bringmann A & Reichenbach A (2009). Purinergic signaling in special senses. *Trends Neurosci* **32**, 128–141.
- Johansson B, Georgiev V & Fredholm BB (1997). Distribution and postnatal ontogeny of adenosine A<sub>2A</sub> receptors in rat brain: comparison with dopamine receptors. *Neuroscience* **80**, 1187–1207.
- Johansson B, Halldner L, Dunwiddie TV, Masino SA, Poelchen W, Giménez-Llort L, Escorihuela RM, Fernández-Teruel A, Wiesenfeld-Hallin Z, Xu XJ, Hårdemark A, Betsholtz C, Herlenius E & Fredholm BB (2001). Hyperalgesia, anxiety, and decreased hypoxic neuroprotection in mice lacking the adenosine A<sub>1</sub> receptor. *Proc Natl Acad Sci USA* **98**, 9407–9412.
- Kaelin-Lang A, Lauterburg T & Burgunder JM (1999). Expression of adenosine A<sub>2A</sub> receptors gene in the olfactory bulb and spinal cord of rat and mouse. *Neurosci Lett* **261**, 189–191.
- Kang D, Hogan JO & Kim D (2014). THIK-1 (K2P13.1) is a small-conductance background K<sup>+</sup> channel in rat trigeminal ganglion neurons. *Pflugers Arch* **466**, 1289–1300.
- Kim CS & Johnston D (2015). A<sub>1</sub> adenosine receptor-mediated GIRK channels contribute to the resting conductance of CA1 neurons in the dorsal hippocampus. *J Neurophysiol* **113**, 2511–2523.
- Kollo M, Schmaltz A, Abdelhamid M, Fukunaga I & Schaefer AT (2014). ‘Silent’ mitral cells dominate odor responses in the olfactory bulb of awake mice. *Nat Neurosci* **17**, 1313–1315.
- Langer D, Hammer K, Koszalka P, Schrader J, Robson S & Zimmermann H (2008). Distribution of ectonucleotidases in the rodent brain revisited. *Cell Tissue Res* **334**, 199–217.
- Lein ES, Hawrylycz MJ, Ao N, Ayres M, Bensinger A, Bernard A, Boe AF, Boguski MS, Brockway KS, Byrnes EJ, Chen L, Chen L, Chen TM, Chin MC, Chong J, Crook BE, Czaplinska A, Dang CN, Datta S, Dee NR, Desaki AL, Desta T, Diep E, Dolbear TA, Donelan MJ, Dong HW, Dougherty JG, Duncan BJ, Ebbert AJ, Eichele G, Estin LK, Faber C, Facer BA, Fields R, Fischer SR, Fliss TP, Frensley C, Gates SN, Glattfelder KJ, Halverson KR, Hart MR, Hohmann JG, Howell MP, Jeung DP, Johnson RA, Karr PT, Kawar R, Kidney JM, Knapik RH, Kuan CL, Lake JH, Laramée AR, Larsen KD, Lau C, Lemon TA, Liang AJ, Liu Y, Luong LT, Michaels J, Morgan JJ, Morgan RJ, Mortrud MT, Mosqueda NF, Ng LL, Ng R, Orta GJ, Overly CC, Pak TH, Parry SE, Pathak SD, Pearson OC, Puchalski RB, Riley ZL, Rockett HR, Rowland SA, Royall JJ, Ruiz MJ, Sarno NR, Schaffnit K, Shapovalova NV, Sivisay T, Slaughterbeck CR, Smith SC, Smith KA, Smith BI, Sodt AJ, Stewart NN, Stumpf KR, Sunkin SM, Sutram M, Tam A, Teemer CD, Thaller C, Thompson CL, Varnam LR, Visel A, Whitlock RM, Wohnoutka PE, Wolkey CK, Wong VY, Wood M, Yaylaoglu MB, Young RC, Youngstrom BL, Yuan XF, Zhang B, Zwingman TA & Jones AR (2007). Genome-wide atlas of gene expression in the adult mouse brain. *Nature* **445**, 168–176.
- Leist M, Rinné S, Datunashvili M, Aissaoui A, Pape HC, Decher N, Meuth SG & Budde T (2017). Acetylcholine-dependent upregulation of TASK-1 channels in thalamic interneurons by a smooth muscle-like signalling pathway. *J Physiol* **595**, 5875–5893.
- Lesage F (2003). Pharmacology of neuronal background potassium channels. *Neuropharmacology* **44**, 1–7.
- Liu S, Shao Z, Puche A, Wachowiak M, Rothermel M & Shipley MT (2015). Muscarinic receptors modulate dendrodendritic inhibitory synapses to sculpt glomerular output. *J Neurosci* **35**, 5680–5692.
- Lohr C, Grosche A, Reichenbach A & Hirnet D (2014). Purinergic neuron-glia interactions in sensory systems. *Pflugers Arch* **466**, 1859–1872.
- Lopes LV, Cunha RA, Kull B, Fredholm BB & Ribeiro JA (2002). Adenosine A<sub>2A</sub> receptor facilitation of hippocampal synaptic transmission is dependent on tonic A<sub>1</sub> receptor inhibition. *Neuroscience* **112**, 319–329.
- Lüscher C & Slesinger PA (2010). Emerging roles for G protein-gated inwardly rectifying potassium (GIRK) channels in health and disease. *Nat Rev Neurosci* **11**, 301–315.
- Mahan LC, McVittie LD, Smyk-Randall EM, Nakata H, Monsma FJ Jr, Gerfen CR & Sibley DR. (1991). Cloning and expression of an A<sub>1</sub> adenosine receptor from rat brain. *Mol Pharmacol* **40**, 1–7.
- Maher BJ & Westbrook GL (2005). SK channel regulation of dendritic excitability and dendrodendritic inhibition in the olfactory bulb. *J Neurophysiol* **94**, 3743–3750.



- Maher BJ & Westbrook GL (2008). Co-transmission of dopamine and GABA in periglomerular cells. *J Neurophysiol* **99**, 1559–1564.
- Manella LC, Petersen N & Linster C (2017). Stimulation of the locus coeruleus modulates signal-to-noise ratio in the olfactory bulb. *J Neurosci* **37**, 11605–11615.
- Meuth SG, Budde T, Kanyshkova T, Broicher T, Munsch T & Pape HC (2003). Contribution of TWIK-related acid-sensitive  $K^+$  channel 1 (TASK1) and TASK3 channels to the control of activity modes in thalamocortical neurons. *J Neurosci* **23**, 6460–6469.
- Najac M, De Saint Jan D, Reguero L, Grandes P & Charpak S (2011). Monosynaptic and polysynaptic feed-forward inputs to mitral cells from olfactory sensory neurons. *J Neurosci* **31**, 8722–8729.
- Nunez-Parra A, Li A & Restrepo D (2014). Coding odor identity and odor value in awake rodents. *Prog Brain Res* **208**, 205–222.
- Parsa PV, D'Souza RD & Vijayaraghavan S (2015). Signaling between periglomerular cells reveals a bimodal role for GABA in modulating glomerular microcircuitry in the olfactory bulb. *Proc Natl Acad Sci USA* **112**, 9478–9483.
- Patel AJ, Honoré E, Lesage F, Fink M, Romey G & Lazdunski M (2001). Inhalational anesthetics activate two-pore-domain background  $K^+$  channels. *Nat Neurosci* **2**, 422–436.
- Rajan S, Wischmeyer E, Karschin C, Preisig-Muller R, Grzeschik KH, Daut J, Karschin A & Derst C (2001). THIK-1 and THIK-2, a novel subfamily of tandem pore domain  $K^+$  channels. *J Biol Chem* **276**, 7302–7311.
- Rebola N, Sebastião AM, de Mendonca A, Oliveira CR, Ribeiro JA & Cunha RA (2003). Enhanced adenosine  $A_{2A}$  receptor facilitation of synaptic transmission in the hippocampus of aged rats. *J Neurophysiol* **90**, 1295–1303.
- Reppert SM, Weaver DR, Stehle JH & Rivkees SA (1991). Molecular cloning and characterization of a rat  $A_1$ -adenosine receptor that is widely expressed in brain and spinal cord. *Mol Endocrinol* **5**, 1037–1048.
- Ribeiro JA & Sebastião AM (2010). Modulation and metamodulation of synapses by adenosine. *Acta Physiol (Oxf)* **199**, 161–169.
- Rieger A, Deitmer JW & Lohr C (2007). Axon-glia communication evokes calcium signaling in olfactory ensheathing cells of the developing olfactory bulb. *Glia* **55**, 352–359.
- Rinberg D, Koulakov A & Gelperin A (2006). Sparse odor coding in awake behaving mice. *J Neurosci* **26**, 8857–8865.
- Rosin DL, Robeva A, Woodard RL, Guyenet PG & Linden J (1998). Immunohistochemical localization of adenosine  $A_{2A}$  receptors in the rat central nervous system. *J Comp Neurol* **401**, 163–186.
- Roux L, Madar A, Lacroix MM, Yi C, Benchenane K & Giaume C (2015). Astroglial connexin 43 hemichannels modulate olfactory bulb slow oscillations. *J Neurosci* **35**, 15339–15352.
- Shusterman R, Smear MC, Koulakov AA & Rinberg D (2011). Precise olfactory responses tile the sniff cycle. *Nat Neurosci* **14**, 1039–1044.
- Sickmann T & Alzheimer C (2003). Short-term desensitization of G-protein-activated, inwardly rectifying  $K^+$  (GIRK) currents in pyramidal neurons of rat neocortex. *J Neurophysiol* **90**, 2494–2503.
- Skatchkov SN, Eaton MJ, Shuba YM, Kucheryavykh YV, Derst C, Veh RW, Wurm A, Iandiev I, Pannicke T, Bringmann A & Reichenbach A (2006). Tandem-pore domain potassium channels are functionally expressed in retinal (Müller) glial cells. *Glia* **53**, 266–276.
- Smear M, Shusterman R, O'Connor R, Bozza T & Rinberg D (2011). Perception of sniff phase in mouse olfaction. *Nature* **479**, 397–400.
- Stavermann M, Meuth P, Doengi M, Thyssen A, Deitmer JW & Lohr C (2015). Calcium-induced calcium release and gap junctions mediate large-scale calcium waves in olfactory ensheathing cells in situ. *Cell Calcium* **58**, 215–225.
- Storace DA & Cohen LB (2017). Measuring the olfactory bulb input-output transformation reveals a contribution to the perception of odorant concentration invariance. *Nat Commun* **8**, 81.
- Svenningsson P, Le Moine C, Kull B, Sunahara R, Bloch B & Fredholm BB (1997). Cellular expression of adenosine  $A_{2A}$  receptor messenger RNA in the rat central nervous system with special reference to dopamine innervated areas. *Neuroscience* **80**, 1171–1185.
- Thyssen A, Hirnet D, Wolburg H, Schmalzig G, Deitmer JW & Lohr C (2010). Ectopic vesicular neurotransmitter release along sensory axons mediates neurovascular coupling via glial calcium signaling. *Proc Natl Acad Sci USA* **107**, 15258–15263.
- Tripathy SJ, Padmanabhan K, Gerkin RC & Urban NN (2013). Intermediate intrinsic diversity enhances neural population coding. *Proc Natl Acad Sci USA* **110**, 8248–8253.
- Uchida N, Poo C & Haddad R (2014). Coding and transformations in the olfactory system. *Annu Rev Neurosci* **37**, 363–385.
- Wei AD, Gutman GA, Aldrich R, Chandy KG, Grissmer S & Wulff H (2005). International Union of Pharmacology. LII. Nomenclature and molecular relationships of calcium-activated potassium channels. *Pharmacol Rev* **57**, 463–472.

## Additional information

### Competing interest

The authors declare no conflict of interest.

### Author contributions

Design of the work: C.L., D.H. and N.R. Acquisition and analysis of data, providing material: C.L., D.H., J.B., K.S., M.B., M.C. N.B., N.R., S.W. and T.F. Writing the manuscript: C.L., D.H., M.C. and N.R. All authors revised and approved the manuscript. All authors agree to be accountable for all aspects of the work in ensuring that questions related to the accuracy or integrity of any part of the work are appropriately investigated and resolved. All persons designated as authors qualify for authorship, and all those who qualify for authorship are listed.

### Funding

Financial support by the Deutsche Forschungsgemeinschaft (LO 779/6-1 and HI 1288/3-1), the Landesforschungsförderung Hamburg (Read Me) and the Swedish Research Council (Dnr: 2016-01381) is gratefully acknowledged.